

## 3ks Specific Impulse with a ns-pulse Laser Microthruster

Claude R. Phipps\* and James R. Luke†  
*Photonic Associates, LLC, Santa Fe, NM 87508*

Wesley D. Helgeson‡  
*NMT/IERA, Albuquerque, NM 87106*

We developed a prototype device which demonstrated the feasibility of using ns-duration laser pulses in a laser microthruster. Using several metallic targets driven by a “microchip” laser, we measured thrust, specific impulse  $I_{sp}$ , specific ablation energy  $Q^*$  and ablation efficiency. Specific impulse is adjusted by varying laser intensity on target. In this way, we were able to vary specific impulse from 200s to 3,800s on gold, with corresponding momentum coupling coefficient  $C_m$  varying from 70 to  $7\mu\text{N}/\text{optical watt}$  and ablation efficiency near 100% at a  $1\text{MJ}/\text{m}^2$  optimum pulse fluence. We will discuss simulations of the laser-target interaction which agreed well with the results obtained on metallic fuel systems. We used a Concepts Research, Inc. microchip laser with 170mW average optical power, 8kHz repetition rate and  $20\mu\text{J}$  pulse energy for many of the measurements. Thrust was in the 100nN -  $1\mu\text{N}$  range for all the work, requiring development of an extremely sensitive, low-noise thrust stand, which is discussed in a companion paper. We will discuss the design of realistic metallic fuel delivery systems. We also report time-of-flight measurements on ejected metal ions, which gave velocities up to 80km/s. Near the optimum fluence, we found good agreement between  $I_{sp}$  deduced from the  $C_m Q^*$  product and from ion velocity  $v_i$ . We saw strong divergence between these two parameters at higher intensity. Relative to the ms-duration thrusters which we have demonstrated in the past, this change offers the use of any target material, the use of more-efficient reflection-mode target illumination, and specific impulse adjustable to match the mission.

Key words: electric propulsion, ns laser microthruster, 3600 second specific impulse

### Nomenclature

$C_m$	= laser momentum coupling coefficient	$Q^*$	= specific ablation energy
$CW$	= “continuous wave”, continuous laser output rather than pulsed	$R$	= radius of thruster attachment point from center of rotation
$DPSS$	= diode-pumped, solid state	$v_E$	= exhaust velocity
$E$	= short for “10 <sup>^</sup> ”	$TEC$	= thermoelectric cooler
$f$	= repetition frequency	$W$	= laser pulse energy incident on test sample
$F$	= thrust	$\Delta m$	= ablated mass
$g_o$	= acceleration of gravity at Earth’s surface	$\eta_{AB}$	= ablation efficiency
$I$	= laser intensity on target	$\eta_E$	= laser optical power out/electrical power in
$I_{sp}$	= specific impulse	$\theta$	= angle of rotation of torsion bar
$k$	= constant relating rotation angle $\theta$ to torque	$\tau$	= laser pulse duration
$ksi$	= tensile strength expressed in $\text{klb}/\text{in}^2$		
$\langle P \rangle$	= average incident laser power		

\* President and General Partner, 200A Ojo de la Vaca Road, [crhipps@aol.com](mailto:crhipps@aol.com). Member AIAA.

† Senior Research Staff Member and Partner, 200A Ojo de la Vaca Road.

‡ Senior Research Associate, 901 University Blvd SE.

## I. Introduction

In earlier work, we showed the feasibility of using ms-duration laser diodes to drive a microthruster based on ablation of solid polymer targets [1, 2]. There were two difficulties identified in that work. One was the necessity of using polymer targets with low thermal conductivity such as PVC, PVN or GAP (no metals could be used) in order to achieve the temperatures necessary for efficient propulsion and minimally acceptable  $I_{sp}$ . The other was the requirement for transmission-mode illumination to avoid target ablation products backstreaming onto the optics [Figure 1]. It was always understood that ns-pulse illumination would eliminate both problems, although at the cost of some loss in power conversion efficiency.

However, ns-pulse diode-pumped fiber laser amplifiers have for some time been capable of electrical efficiency

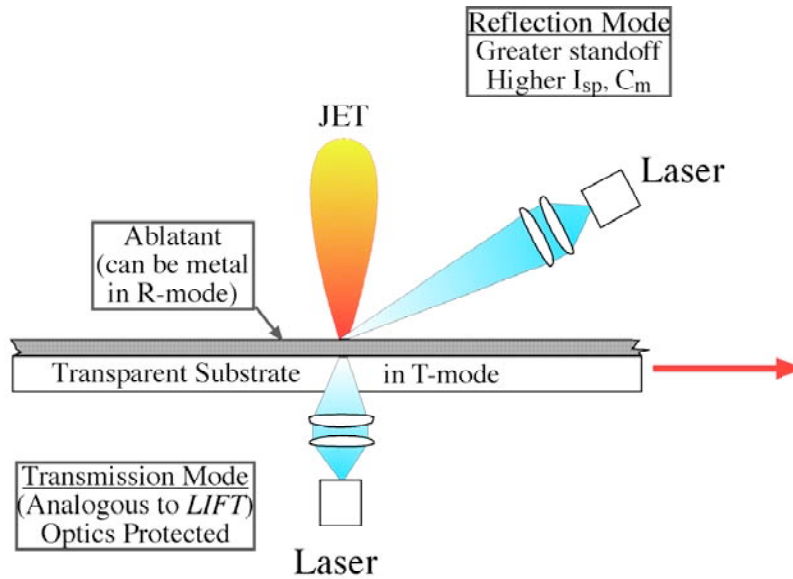


**Figure 1. Transmission (T) vs. reflection (R) mode illumination.** Nanosecond-pulse illumination permits using R-mode illumination in laser ablation propulsion, a definite advantage for simplicity of targets and optics, as well as laser energy deposition efficiency.

with simple desktop-scale ns-duration lasers using metallic targets in vacuum.

In this paper, we will describe measurements of thrust, specific impulse and energetic efficiency in laser propulsion with ns-duration pulses which were made for the first time using a completely self-contained microthruster suspended in a torsion-type thrust stand capable of 25nN precision in measuring thrust. Intensity on target was in the  $PW/m^2$  range. Performance of the test stand is described in a companion paper in this conference.

## II. Definition of Terms

For the sake of simplicity, we will consider a monoenergetic laser-produced plasma jet with exhaust velocity  $v_E$ . We have shown that this approximation will not introduce large errors [ $\langle v^2 \rangle / \langle v \rangle^2 \approx 1.15$ ] for typical laser-produced plasma jets, and the principal points we want to make here will be made more transparently using that assumption. We define the laser momentum coupling coefficient  $C_m$  as:

$$C_m = F / \langle P \rangle = \Delta m v_E / W. \quad (1)$$

In the ablation process,  $Q^*$  joules of laser light are consumed per kg of ablated mass, and  $C_m$  units of impulse  $\Delta m v_E$  are produced. The product of  $C_m$  and  $Q^*$  is the exhaust velocity  $v_E$  of the ablation stream, given the monoenergetic assumption. This can be seen from the definitions of  $C_m$  and  $Q^*$ :

$$C_m Q^* = (\Delta m v_E / W)(W / \Delta m) = v_E, \quad (2)$$

$\eta_E = 10\%$  [3], so the conversion efficiency sacrifice is not prohibitive for the technology now, and can only improve in the future. Also, fiber lasers are low-mass devices, unlike conventional DPSS lasers.

In contrast, microchip lasers [4] currently have  $\eta_E = 1-2\%$  a figure which is primarily due to the power consumed by the TEC which is required to stabilize operating temperature of the laser chip.

The energetic advantages of ns-duration and shorter pulses for manipulating objects in space via laser ablation propulsion were pointed out in [5] and the possibility of using onboard microchip lasers for ns-duration propulsion was discussed in [4,6]. In [6],  $I_{sp}$  up to 4.9ks was reported using this technique. Other measurements going back several decades have shown [7,8] that  $I_{sp}$  values from 7 to more than 25ks are readily obtained

independent of the ablation efficiency. If for example, a significant amount of the incident energy is absorbed as heat in the target substrate rather than producing material ejection,  $Q^*$  will be higher, but  $C_m$  will be proportionately lower, giving the same velocity in the end. In propulsion work, “specific impulse”  $I_{sp}$  is customary notation for  $v_E/g_0$ , and we define  $I_{sp}$  as

$$I_{sp} = C_m Q^* / g_0 \quad (3)$$

Energy conservation prevents  $C_m$  and  $I_{sp}$  from being arbitrary. Increasing one decreases the other. Energy conservation requires that several constant product relationships exist:

$$2\eta_{AB} = \Delta m v_E^2 / W = C_m^2 Q^* = g_0 C_m I_{sp} = C_m v_E \quad (4)$$

The ablation efficiency parameter  $\eta_{AB}$  in Eq. (3) is the ratio of exhaust kinetic power to incident laser power  $\langle P \rangle$ . The definition allows  $\eta_{AB} > 1$  for exothermic targets. For nonexothermic “passive” targets,  $\eta_{AB} \leq 1$  and the product

$$C_m I_{sp} \leq 2/g_0 = 0.204. \quad (5)$$

### III. Microthruster Design and Test Setup

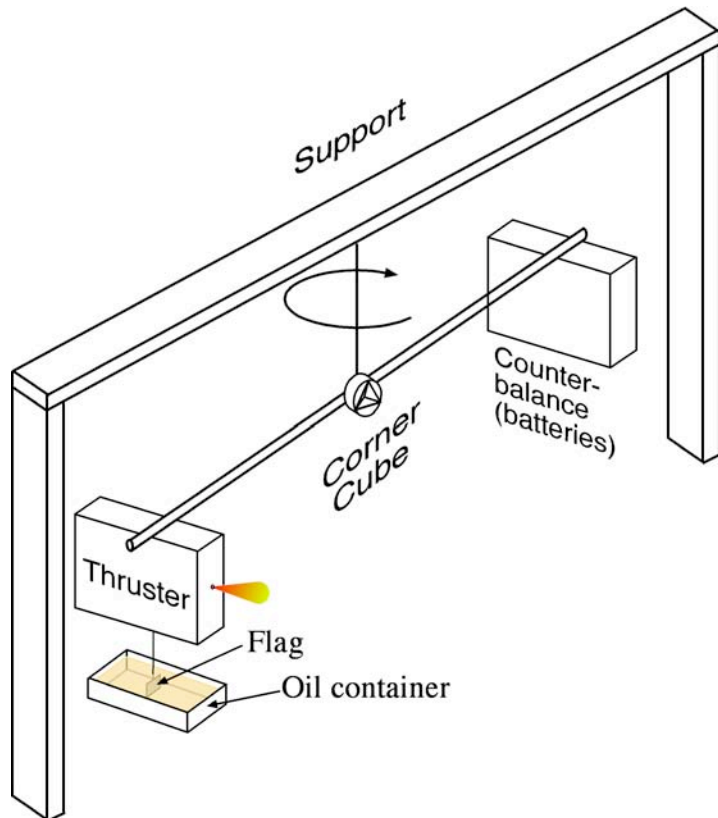


**Figure 2. Vacuum thrust stand setup.** Power supply is on board the thrust measurement bar with the thruster, and command and data transfer uses an IR data link, so that the only mechanical connection with the outside world is the 254- $\mu$ m diameter steel fiber supporting the bar. An interferometer based on a solid glass retroreflecting “corner cube” (described below) is the key to resolving rotation of the bar. Critical damping is provided by a flag immersed in diffusion pump oil.

In order to test our concepts fully, it was necessary to build a test microthruster which could accommodate various target materials with features including a target delivery system providing several hours of operating lifetime, power supply and infrared data link, all completely self-contained and isolated from the external world except for the torsion fiber which provided restoring force in the thrust-measurement apparatus [Figure 2]. The vacuum thrust stand setup was identical to the device reported in [1] except for a) 40-cm rather than 10-cm torsion fiber length, b) the critical damping attachment and c) the interferometer element in the center of the support bar. The latter replaces the simple mirror used as a rotation readout in [1]. The entire setup mounted inside the vacuum test chamber. For this system, thrust  $F$  is given by

$$F = k\theta/R \quad (6)$$

In our case,  $k = 194$  pN-m/ $\mu$ rad and  $R = 0.155$ m, so that  $k/R = 1.25$ nN/ $\mu$ rad. The rotation sensor resolved 20 $\mu$ rad bar rotation to deliver 25nN precision.

A separate design challenge was to develop a means of delivering laser energy to the system through the vacuum chamber envelope from two different benchtop laser systems while the apparatus was rotating in the test chamber. Our solution to this problem is shown in Figure 3.

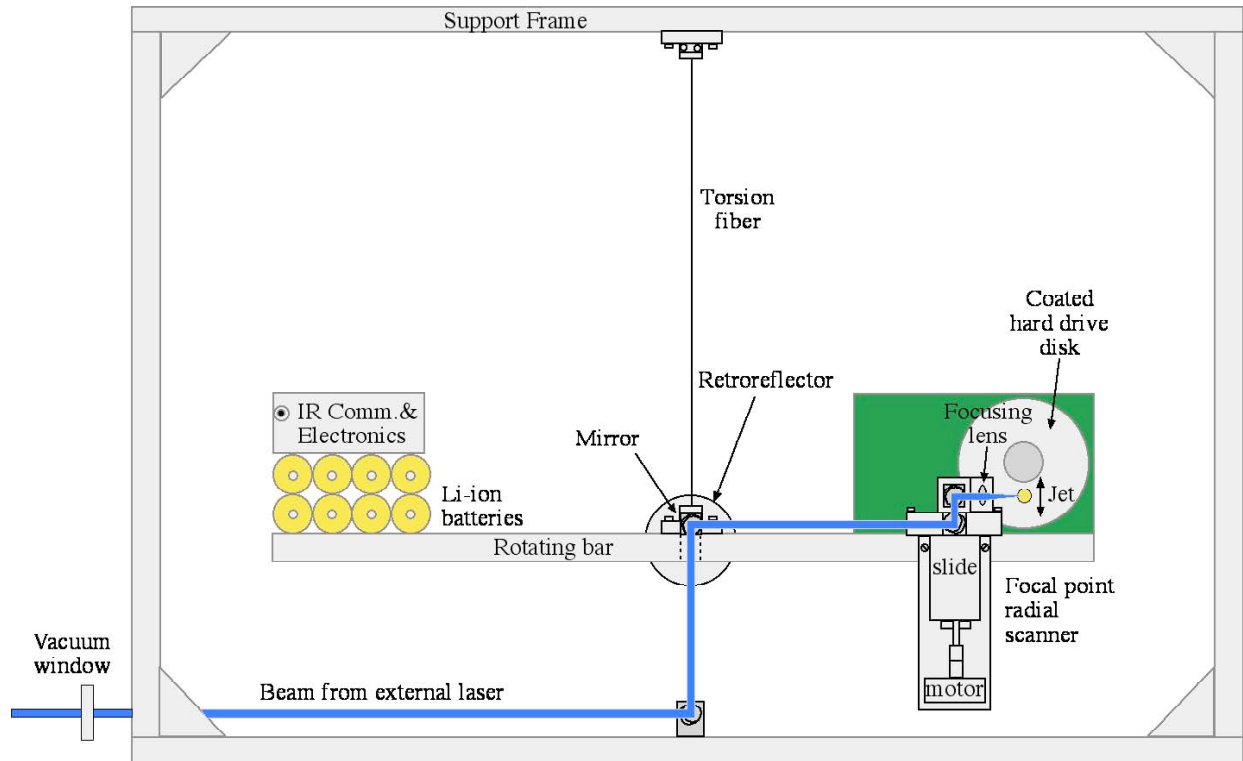


**Figure 3. Design for ns-pulse thrust measurements.** The steel fiber which was the core of the instrument was a 40-cm long strand of 250 $\mu$ m, 500ksi steel “rocket wire” provided by MJ Wire, Inc. The hard drive was an IBM DKLA 22160 with a 2.5 inch diameter disk operating at 4200 rpm. An IR communication link with a Labview® interface that we developed handled data and commands. Input optical power levels ranged from 10 to 100mW.

Although operating conditions were sometimes deliberately chosen otherwise (e.g., for measurements of surface

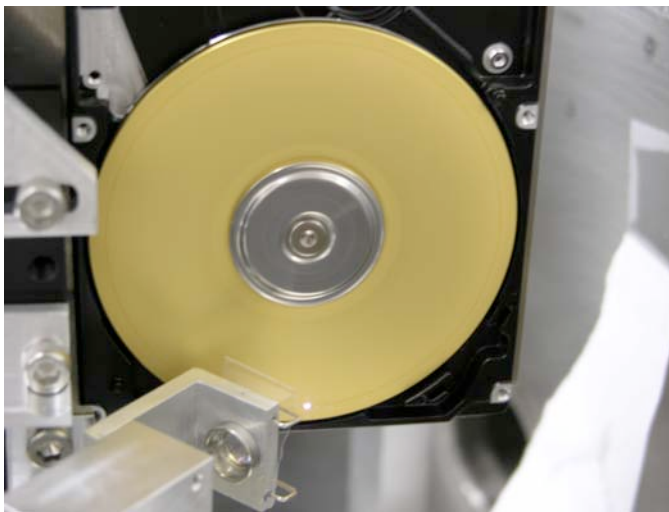


**Figure 4. Au coating.** Electroplating was by far the most successful coating technique. Thruster jet is visible at bottom of spinning disk.

regularity obtained in laser planing of the surface), thrust data runs with the device were always set up with a radial scan speed sufficient to insure single-spot irradiation of any target site on the spinning fuel disk. There have been some successes and some failures in our attempts to coat the disks. Delamination was seen with Zr coatings which were applied by ion sputtering, but Al coatings applied in this way were of good quality, although considerably thinner (1-2 $\mu$ m vs. 20 $\mu$ m). The causes of the problems with the Zr coatings have not been identified. We had the best results with gold electroplating. The coating was thick, tough and adherent, giving hours of good performance in tests (Fig. 4). A typical fuel disk would have lasted for 350 hours of continuous operation at the 10-100mW input optical power levels that we used for tests, or 5 hours at the 8W level we would propose for a space-qualified microthruster capable of generating 80 $\mu$ N thrust.

Two different lasers were employed to provide the optical input for tests (Table 1). This was necessary because the Concepts Research microchip laser was incapable of generating the maximum intensities that we required. However, its 8kHz output format was the same as that of the fiber laser we plan to use in future work, and we felt that we should use it for as much of the data as possible. The Quantel laser was a standard flashlamp-pumped Nd:YAG tabletop unit.

Laser	Quantel	Concepts Research
Pulse energy (mJ)	1-20	0.0132
Pulse repetition rate (Hz)	10	8000
Power on target (mW)	10-220	106
Beam quality factor $M^2$	3.6	1.2
Spot size on target ( $\mu\text{m}$ )	20-60	5-20
Fluence on target ( $\text{J}/\text{m}^2$ )	3E6-6E7	1-3E5
Pulse duration (ns)	4.55	4.0
Intensity on target ( $\text{TW}/\text{m}^2$ )	660-14,000	20-65
Typical radial velocity ( $\mu\text{m}/\text{hr}$ )	700	

To get the range of intensities we wanted to study, a beam from either of two lasers (Table 1) was directed to the disk by a 15-mm focal length lens. Beam incidence angle on the disk was 45 degrees. Spot sizes on target varied, as did the laser pulse energy, which was controlled by absorptive attenuators. Given the  $M^2$  value for the Quantel laser (Table 1), the smallest spot we could expect was  $20\mu\text{m}$ . Typical laser spot diameter on target was  $40\mu\text{m}$ , determined by microscopic examination.

An optical link operated with Labview® turned the disk drive on and off, and commanded the transverse drive to move the lens across the disk in a radial direction at a velocity  $v_r$  which could be adjusted from  $1\mu\text{m}/\text{hr}$  to  $8,000\mu\text{m}/\text{hr}$ . This was normally set to about  $700\mu\text{m}/\text{hr}$  to avoid overlap even for our largest illumination spots.

The disk drive motor was operated by a bank of Li-ion batteries which also served as counterweight for the thruster. These were capable of powering the system, including the transverse drive and the optical communication link, for up to three hours. We found that it was necessary to momentarily turn the transverse drive stepper motor off when measuring thrust, because of the interaction between the motor's magnetic field and the Earth's field.

Typical operating pressure for tests was  $30\mu\text{torr}$ .

Material	Gold		Aluminum	
	Fluence ( $\text{J}/\text{m}^2$ )	6.36E5	2.08E7	3.46E5
Intensity ( $\text{W}/\text{m}^2$ )	1.40E14	4.57E15	7.60E13	2.37E13
Thrust ( $\mu\text{N}$ )	0.63	0.47	0.94	1.88
$C_m(\mu\text{N}/\text{W})$	68	7.2	111	32
$Q^*(\text{kJ}/\text{kg})$	5.28E5	5.90E5	9.79E4	2.71E5
$I_{sp}(\text{s})$ from $C_m Q^*$	3660	212	1120	520
$\eta_{AB}(\%)$	100	0.75	61	8.1
Test duration (m)	120	16	120	24.25
$v_i$ from TOF (m/s)	3.59E4	7.75E4	6.48E4	8.05E3
$I_{sp}$ from $v_i$	3664	7905	6610	822
Test ID	BT12§	BT8§	9A§	4§, 17§

#### IV. Thrust Measurements

Ion time-of-flight (TOF) data reported in Table 2 is discussed in more detail in section V following. Figures 5 and 7 show the results we obtained for thrust,  $C_m$ ,  $I_{sp}$  and  $\eta_{AB}$  for the Al and Au target disks vs. incident intensity.

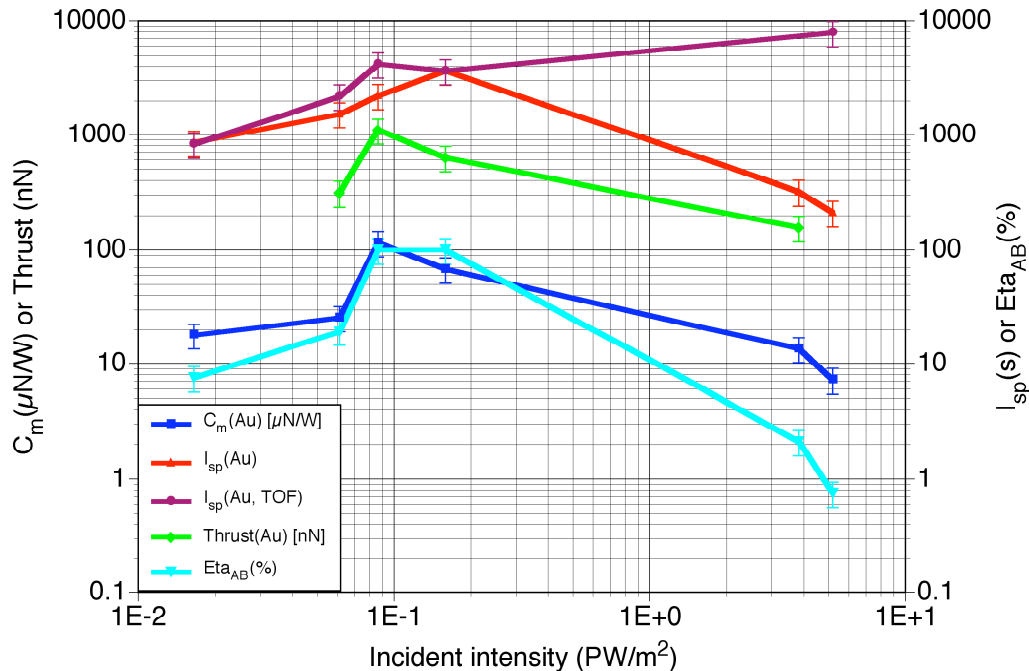


**Figure 5. Experimental data for Au target vs. incident intensity.** Ablation efficiency approaches 100% near 100 GW/m<sup>2</sup>. Thrust as small as 150nN was measured reliably.  $C_m$  ranged between 10 and 100  $\mu$ N/W. Specific impulse based on measured mass loss was as large as 3,700 seconds, and could be varied between 0.2 and 3.7 ks by varying incident intensity.  $I_{sp}$  based on ion TOF measurements agrees roughly with  $I_{sp}$  from mass loss up to 150 GW/m<sup>2</sup>, but the two trends diverge at higher intensity, as ablation efficiency drops to the 1% level.

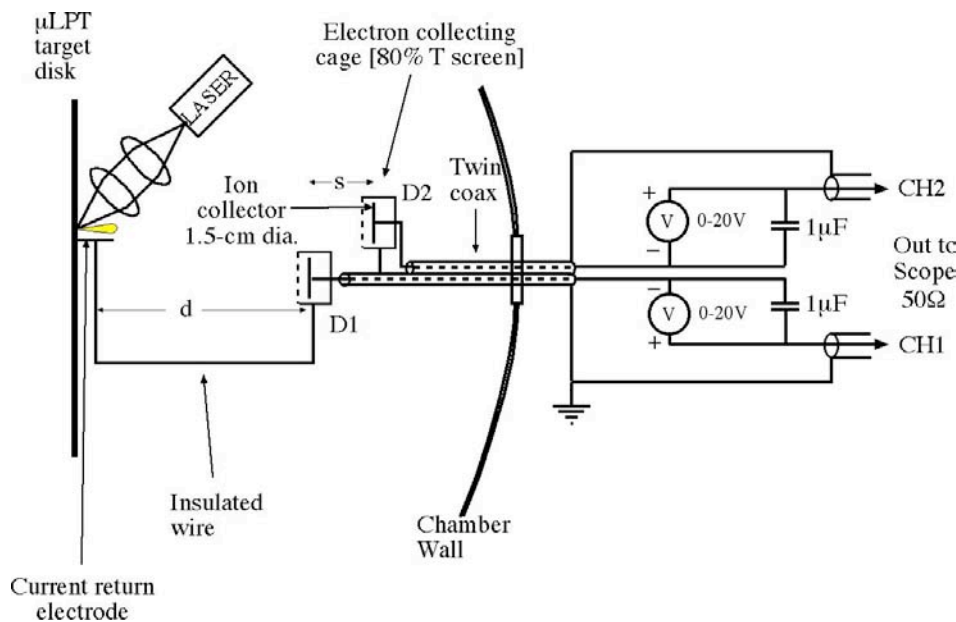


**Figure 6. Twin Ion Time-of-flight Detectors** were typically maintained at  $-10$ V bias to select ions and reject electrons to the 80% transmission screen covering the detector. A current return electrode was necessary because the source (the jet) is not grounded. Distance  $d$  is the separation of D1 from the source (5.8cm) and  $s$  is the mutual separation between D1 and D2 (2.8cm).

Simulations that we did of the laser target interaction gave essentially the same fluence for maximum ablation efficiency as was observed in the Au data [ $1\text{MJ}/\text{m}^2$ ].

Al data [Figure 6] was not as complete as the Au data because the 1-2 $\mu$ m thickness of the Al coatings did not permit reaching the higher intensities before coating burnthrough occurred.

## V. Time-of-Flight Measurements

We installed a pair of shielded Langmuir/Faraday time-of-flight detectors in the chamber as shown in

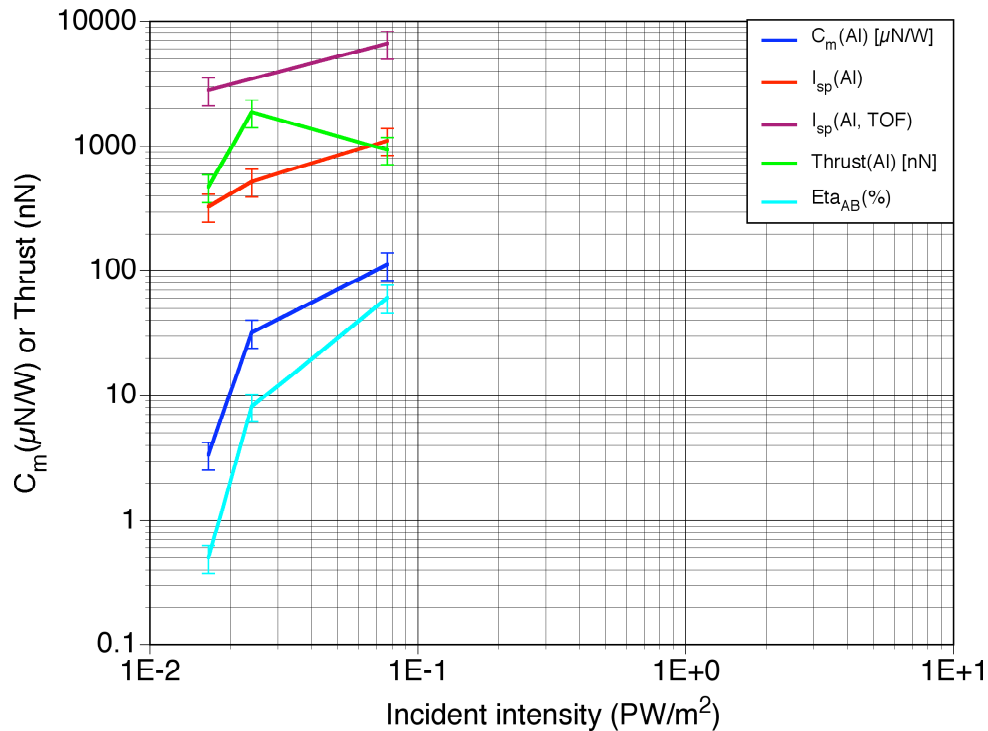


**Figure 7. Experimental data for Al target vs. incident intensity.** Ablation efficiency approaches 100% near 100 GW/m<sup>2</sup>. C<sub>m</sub> ranged between 5 and 100 μN/W. Specific impulse based on measured mass loss was as large as 1,100 seconds. I<sub>sp</sub> based on ion TOF measurements did not agree with I<sub>sp</sub> from mass loss up to 150 GW/m<sup>2</sup>, being much larger for the entire range studied. Higher intensities could not be studied because of Al coating burnthrough.

Figure 6. For all the work reported here, the dimensions d and s were 5.8 and 2.8 cm, respectively.

These choices of separation gave good signal strength and still provided adequate velocity resolution for the ion speeds we expected to find, in the range  $2E4 < v_i < 1E5$  m/s [ $2E3 < I_{sp} < 1E4$ ].

For ion velocity measurements, we biased the probes so that only ions were collected. We found that  $V = -10V$  was sufficient to do this.

The two signals were recorded on a Tektronix 3014B digital storage oscilloscope. A typical TOF trace for moderate laser fluence is reproduced in Figure 8. Figure 9 shows a high-fluence TOF trace.

We irradiated one track on the gold target disk for 40 minutes to see whether the bottom of the feature created would be too rough to maintain focus. Microscopic examination showed that the irradiated surface was smoother than the original surface. The rms roughness could not be directly determined, but was better than  $\pm 1 \mu m$ .

## V. Summary and Conclusions

We measured, for the first time, the thrust developed when ns-duration, repetitive laser pulses are directed at a metal target material in vacuum in a completely self-contained thruster device. To do the measurements, with our laboratory lasers, it was necessary to measure (for the first time) thrusts as small as 100nN with 25% accuracy using a new type of thrust stand that we invented for the measurements.

We showed that a ns-pulse laser-driven microthruster can reach I<sub>sp</sub> values in excess of 3ks on a sustained basis, and that I<sub>sp</sub> can be adjusted over a decade by varying laser intensity.

We measured ablation efficiencies up to 100% with passive (nonexothermic) metallic targets. These were gold and aluminum coatings applied to a 2.5-inch IBM hard drive disk. Electroplated Au coatings were thicker than the Al coating that could be applied by ion sputtering, with the result that burnthrough prevented taking Al data at the highest intensities employed.

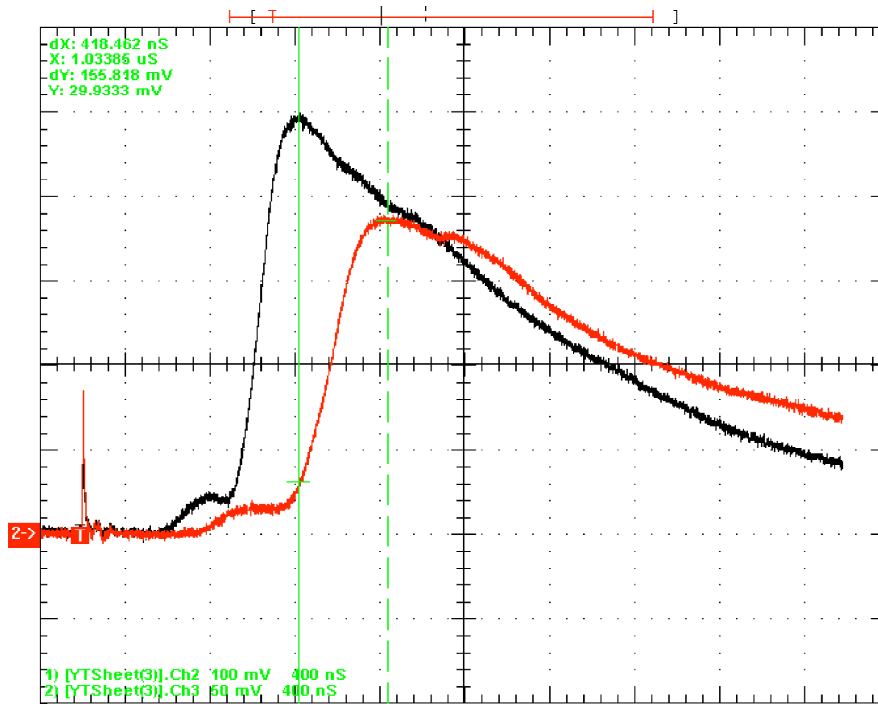


**Figure 8. Moderate Fluence TOF Detector Trace (-10V bias, Au Target)** shows ion speed 67km/s at the waveform peaks and 76km/s at the half-height of the rise. The two traces are derived from D1 and D2 in Figure 6, which are separated by 2.8cm. This corresponds to ion  $I_{sp} = 6.84$  and  $7.75$  ks, respectively, corresponding to the  $0.09\text{PW}/\text{m}^2$  data point in Figure 5. Laser fluence on target was  $0.35\text{MJ}/\text{m}^2$  [near the optimum  $1\text{MJ}/\text{m}^2$  fluence value], and pulse duration was  $4.5\text{ns}$ .

We measured ion velocities using specialized TOF detectors. The simple shape of the detected signals (no multiple peaks) at moderate laser fluence indicated that the TOF signal is produced by a single ion type and a single ion charge state. At higher fluences, we see double-humped TOF signals, which may be due to two different charge states, or due to the plasma clamping phenomenon [9].

The excellent agreement we observed between  $I_{sp}$  deduced from the  $C_m Q^*$  product and from ion velocity  $v_i$  near the optimum fluence of  $1\text{MJ}/\text{m}^2$  tells us that most of the thrust at that fluence is generated by ions, rather than neutrals. The divergence between these two  $I_{sp}$  parameters at higher intensity with Au, and at all intensities for our Al measurements, suggests plasma clamping, a phenomenon in which, above a certain threshold, laser-produced plasma self-regulates its optical transmission in such a way that the fluence transmitted to the surface is constant, independent of incident fluence. This phenomenon will give an initial burst of high-energy ions, but a much lower energy exhaust during the rest of the laser pulse, and could explain the double-humped feature in Figure 9.

There are two other possible reasons for double-humped TOF distributions: a) exciting metal ions to more than one charge state, and b) Surface cleaning of water vapor in the early part of a data run. We have occasionally seen this effect. Possibility a) could not be tested because we did not have charge state diagnostics.

These two  $I_{sp}$  features, which we might call realistic vs. theoretical  $I_{sp}$ , remind us that many reports in the literature of very high  $I_{sp}$  values based on ion velocities alone must be taken with a grain of salt. Ours are the first results reported in the literature in which  $I_{sp}$  was actually measured from mass loss, and the  $C_m Q^*$  product compared with measured ion velocities under the same conditions in the same experiment at appropriate background pressure for measuring ion velocities via TOF. It is also the first in which an optimum fluence for high  $I_{sp}$  was shown.

The fluence for which these two types of  $I_{sp}$  were found to agree,  $1\text{MJ}/\text{m}^2$ , was predicted by our theoretical calculations in reference 10. This fluence corresponds to  $1\text{mJ}$  incident on a  $35\text{-}\mu\text{m}$  spot diameter. This establishes the operating parameters for the fiber laser we would use for a space-qualified microthruster. A pulse energy of  $1\text{mJ}$  at  $16\text{kHz}$ , producing  $8\text{W}$  average power and  $80\mu\text{N}$  thrust, is now very achievable in fiber laser technology, and such a spot size would be easy to achieve with a relatively long focal length lens.

We operated the microthruster for 7 hours on our gold disk target, using about 20% of the target surface, but only about 2% of the target material, which was originally deposited on the disk in a  $20\text{-}\mu\text{m}$ -thick coating. The disk

drive operated at 4200 rpm for 10.4 hours in vacuum without special preparation, and without any degradation in performance. However, this is not the target delivery mechanism we would propose for a space-qualified ns-pulse microthruster.

Taken together, these results demonstrate the feasibility of a ns-pulse laser-driven microthruster, and provide the first data on performance of such a device.

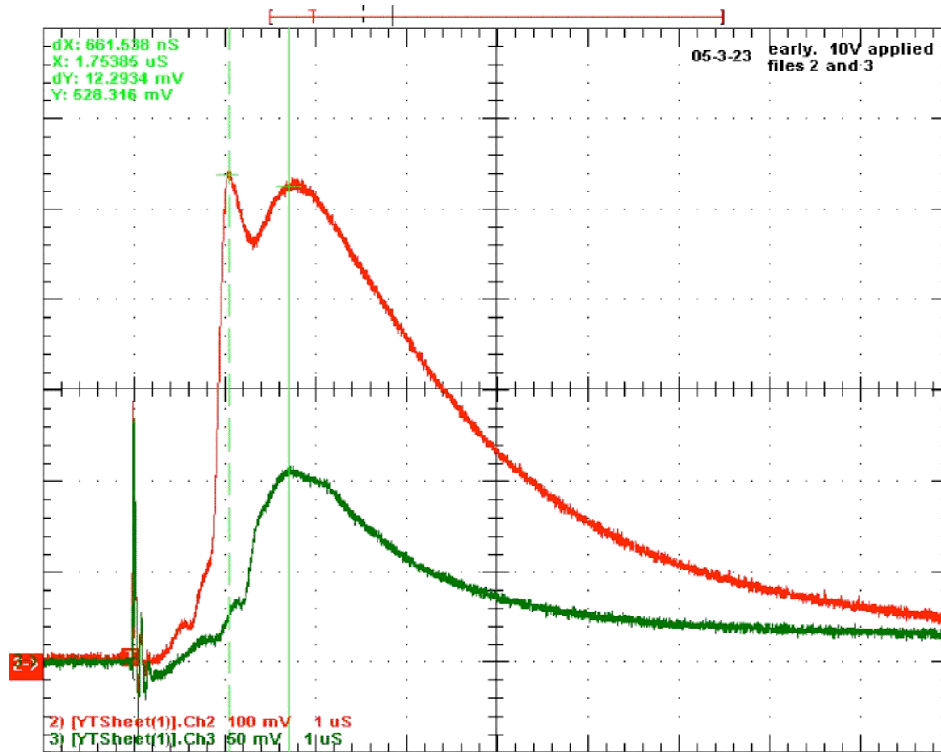


**Figure 9. High fluence TOF Detector Trace (-10V bias, Au Target)** shows ion speed 79km/s at the half-height of the rise in the main feature. This corresponds to ion  $I_{sp} = 8.07$  ks. Unlike the moderate-fluence picture in Figure 8, the TOF distribution has a definite second feature. For this shot, laser fluence on target was  $21\text{MJ}/\text{m}^2$  [above the optimum  $1\text{MJ}/\text{cm}^2$  fluence value], and pulse duration was 4.5ns.

## References

1. Phipps, C. R. and Luke, J. R., "Diode Laser-driven Microthrusters: A new departure for micropropulsion," *AIAA Journal* **40** no. 2 2002, pp. 310-318
2. Phipps, C. , Luke, J., Lippert, T., Hauer, M. and Wokaun, A., "Micropropulsion using a Laser Ablation Jet," *J. Propulsion and Power*, **20** no. 6, 2004, pp. 1000-1011
3. F. di Teodoro, J. P. Koplow and S. W. Moore, "Diffraction-limited, 300-kW peak-power pulses from a coiled multimode optical fiber," *Opt. Lett.* **27**, pp. 518-520 (2002)
4. D. A. Gonzales and R. P. Baker, "Microchip Laser Propulsion for Small Satellites," paper AIAA 2001-3789, 37<sup>th</sup> AIAA/ASME/SAE/ASEE Joint Propulsion Conference, Salt Lake City (2001)
5. C. R. Phipps, "Advantages of using ps-pulses in the ORION Space Debris Clearing System", *Proc. International Conference on Lasers 97*, STS Press, McLean, VA (1998) pp. 935-941
6. D. A. Gonzales and R. P. Baker, "Micropropulsion using a Nd:YAG microchip laser," *Proc. SPIE Conference on High Power Laser Ablation IV*, **SPIE 4760**, pp. 752-765 (2002)
7. C. R. Phipps and M. M. Michaelis, "Laser Impulse Space Propulsion," *Laser and Particle Beams*, **12** (1), 23-54 (1994)
8. D. W. Gregg and S. J. Thomas, "Kinetic Energies of Ions Produced by Laser Giant Pulses", *J. Appl. Phys.* **37**, 4313-16 (1966)

9. J. F. Figueira, S. J. Czuchlewski, C. R. Phipps, Jr., and S. J. Thomas, "Plasma-Breakdown Retropulse Isolators for the Infrared," *Appl. Opt.* **20**, 838 (1980).
10. C. R. Phipps, "Precision Propulsion Concepts for Microsatellites," SBIR Phase I Final Report, TR-2005-0028, available from AFRL/PRS, 1 Pollux Drive, Edwards AFB, CA 93524-7048